Journal of Materials Science: Materials in Electronics (2019) 30:13209–13216
https://doi.org/10.1007/s10854-019-01684-4

Synthesis of CuO–ZnO composite nanoparticles by electrical explosion of wires and their antibacterial activities

A. S. Lozhkomoev[1] · O. V. Bakina[1] · A. V. Pervikov[1] · S. O. Kazantsev[1] · E. A. Glazkova[1]

Received: 2 April 2019 / Accepted: 10 June 2019 / Published online: 18 June 2019

Abstract
Therefore, researchers devote special attention to the search of new composite nanoparticles for biomedical applications. In this research CuO–ZnO composite nanoparticles was synthesized by electrical explosion of cooper and zinc wires in oxygen containing atmosphere. The atomic ratio of metals in the nanoparticles was regulated by varying the wire diameters. The as-synthesized nanoparticles were characterized by powder x-ray diffraction analysis, transmission electron microscopy, energy-dispersive x-ray spectroscopy techniques, sedimentation method, micro electrophoresis and adsorption of nitrogen (BET method). The particles are mostly spherical or close to spherical shape. In the x-ray diffraction patterns of the synthesized nanoparticles the main reflexes correspond to the phases of ZnO and CuO. Furthermore, antibacterial activity of ZnO–CuO nanoparticles against *Escherchia coli* (ATCC 25922) and MRSA (ATCC 43300) were studied, using agar diffusion test and micro dilution assay. Theses result showed synthesized CuO–ZnO nanoparticles have efficient antibacterial activity against gram positive and gram negative bacteria and exceed the antibacterial activity of ZnO and CuO nanoparticles.

1 Introduction

Recently, many researchers pay much attention to synthesis and study of composite multicomponent metal-oxide nanoparticles with enhanced antibacterial activity and biocompatibility. This is due to the fact that alternative methods are being actively sought at present to fight antibiotic and biocide resistant bacteria. As early as 1998 Chapman [1] described bacteria acquired resistance to wide range of preservatives and disinfectants. Moreover, emergence of bacteria resistant strains negatively impacts on water environment, hospital environment, food industry [2–4].

Metal-based nanoparticles are novel antibacterial alternative which exhibit enhanced bactericidal properties [5]. A great deal of interest in composite nanoparticles (CNPs) was generated by their unique properties including not only components additive effect but also synergetic one [6–8]. Physicochemical parameters of the metal components are altered which may lead to novel reactivity towards living organisms. This can alter CNPs activity towards bacteria, enhance antibacterial properties [9]. Cu/TiO_2 [10], AlOOH–Ag [11], noble metal - ZnO [12] nanoparticles and nanostructures with enhanced antibacterial properties have been synthesized.

In the context of the problem, the synthesis and use of CNPs based on copper and zinc oxides can be promising. Both CuO and ZnO are known to have exhibit antibacterial activity [13, 14]. The oxides also are biocompatible and are of low toxity and cost. Carbone et al. [15] showed that mixed oxide $Cu_{0.73}Zn_{0.27}O$ have more pronounced antibacterial effect than the single oxides. $Cu_{0.05}ZnO_{0.95}$ nanoparticles less than 40 nm in size have been prepared by coprecipitation from corresponding nitrate precursors but assessment of the antibacterial activity was not carried out. CuO/ZnO CNPs 15–20 nm in size at a concentration 200 µg/mL prepared by coprecipitation from hyrdroxycarbonate precursors [16] have shown to inhibit *E. coli* growth. Double precipitation technique was used to synthesize CuO/ZnO CNP with hexagonal wurtzite-monoclinic phase morphology [17]. *E. coli* lysis zones for the CNPs with 0.5 g weight reached 20 mm. CuO/ZnO CNPs were synthesized also by sol–gel method [18], electrospinning technique [19], deposition of ZnO on the surface of CuO nanowires [20], green synthesis in *Mentla longfolia* leaf extract [21].

In the present study, we report new method for production of CuO/ZnO CNPs with different components ratios

✉ O. V. Bakina
ovbakina@ispms.tsc.ru

[1] Institute of Strength Physics and Materials Science of Siberian Branch Russian Academy of Sciences (ISPMS SB RAS), 2/4, pr. Akademicheskii, Tomsk, Russia 634055

by simultaneous electric explosion of Cu and Zn wires in oxygen containing atmosphere. The effects of varying the Cu–Zn atomic ratio on the antibacterial properties have been investigated and the results are discussed in this paper.

2 Materials and methods

2.1 Perparation of CuO–ZnO, CuO and ZnO nanoparticles

CuO/ZnO CNP were prepared by the wire electric explosion (EEW) method in argon-oxygen gas mixture (80 volume percent Ar and 20 volume percent O_2), the pressure of the gas mixture being 3×10^5 Pa. Electric circuit diagram of the EEW device is given in Fig. 1. The twisted copper and zinc wires were used to prepare CuO–ZnO nanoparticles. Cu–Zn atomic ratio in samples prepared was determined by values of wire diameters d_1 and d_2.

The device operates in a following way. Energy capacitive storage (*C)* is charged with the power supply (*PS)* to the preset voltage U_0 measured by kilovoltmeter (*kV).* Metal wire is wound on a coil *1* and placed in tight chamber *2*. The wire moves continuously towards the grounded electrode *4* by feed mechanism *6*. The length of the wire exploded corresponds to the distance between grounded electrode *4* and high voltage electrode *3*. The wire reaching grounded electrode *4,* the discharge arrangement operates and high current pulse with density ~ 10^7 A/cm^2 flows. Under the action of the current pulse with duration 1…2 μs the wires explosive destruction takes place. Current and voltage time dependencies are recorded using voltage divider R_2–R_3 and current shunt R_4.

Aerosol containing nanoparticles is taken out of chamber *2* using a fan *7*. CNP are precipitated in the separator *8* under action of the centrifugal force. Purified gas mixture re-enters the chamber *2*. Frequency of the explosions in the experiments is 20 explosions per minute.

Parameters specified for the preparation of CuO–ZnO, CuO and ZnO nanoparticles are listed in Table 1. The parameters listed provide value of the energy introduced into wire corresponding energy being equal 1,8÷2,4 of sublimation energy.

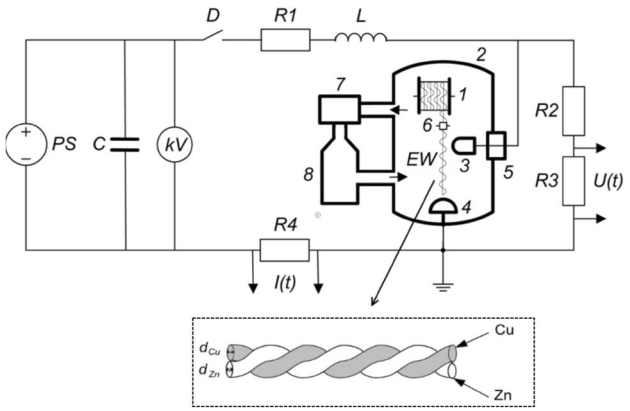

Fig. 1 Circuit diagram of the facility employed for the production of CuO–ZnO nanoparticles

2.2 Characterization of nanoparticles

The resulting samples were characterized by x-ray diffraction (XRD) in a Shimadzu XRD 6000 diffractometer operating with Cu Kα radiation at 40 kV and 30 mA in scanning mode in the range of angles 2θ from ~ 20 to 80° with a step width of 0.02°. Qualitative phase analysis was carried out with powder diffraction file database PDF-2 Release 2014. Nanoparticles morphology and size distribution were studied by transmission electron microscopy (JEM-2100, JEOL, Japan) with integrated energy-dispersive x-ray spectroscopy (EDS) system X-Max (Oxford Instruments, GB). Agglomerates size distribution of the nanoparticles were obtained by the sedimentation method using CPS DS24000 disc centrifuge (CPS Instruments,

Table 1 Parameters of the EEW experiments

Sample[a]	Wire material	d_w, mm	l_w, mm	N, at%	C, μF	U_0, kV
ZnO^{92}–CuO^{8}	Zn	0.38	90	92	3.2	24
	Cu	0.10		8		
ZnO^{74}–CuO^{26}	Zn	0.38	90	74	3.2	28
	Cu	0.20		26		
ZnO^{50}–CuO^{50}	Zn	0.38	90	50	3.2	33
	Cu	0.30		50		
ZnO	Zn	0.38	90	99.9	3.2	22
CuO	Cu	0.37	80	99.9	3.2	29

d_w exploded wires diameter, l_w exploded wire length, N metal ratio in wire, C energy storage electric capacitance, U_0 voltage preset

[a]Atomic ratio of Zn or Cu in CNPs

Prairieville, LA, USA). Zeta potential measurements were performed in deionized water at 25 °C and various pH values using Zetasizer Nano ZSP instrument equipped with an auto-titration unit MPT-2 (Malvern Instruments Ltd, GB) with use of Zetasizer Software.

2.3 Antibacterial activity determination

The antibacterial effect was determined by the viable counts method and agar diffusion test methods using bacteria *E. coli* ATCC 25922 kindly provided by the Russian National Collection of Industrial Microorganisms and methicillin-resistant *Staphylococcus aureus* (MRSA) ATCC 43300 kindly provided by BioVitrum (Novosibirsk, Russia). We adjusted the bacterial suspension to achieve a turbidity equivalent to a 0.5 McFarland standard (Densilameter II, ERBA Lachema). This results in a suspension (*stock solution*) containing approximately 1.5×10^8 colony-forming units (CFU)/mL. The optical density (OD) of *E. coli* suspension was 0.3111, the OD of MRSA suspension was 0.2823.

For agar diffusion test, 20 mL of Mueller–Hinton agar was poured into sterile Petri dishes (diameter 55 mm) and let to solidify. After solidification, wells were made using sterile cork borer. Using a micropipette, 200 µL of nanoparticles water suspension (100 µg/mL) was poured into these wells. Petri dishes were incubated at 37 °C for 24 h. The antibacterial activity was determined by measuring the diameters of inhibition growth zones.

To evaluate the antibacterial activity the viable counts method was used also. In this method, in vitro killing dynamics of bacteria by the nanopowder was measured by counting the residual bacteria in comparison with the starter. A bacterial suspension in phosphate buffered saline (PBS) with the concentration of 10^5 CFU/mL was prepared by dilution of the stock solution. 30 mg of the tested powder were added to 30 mL suspension contained in a sterile conical tube and incubated at room temperature under stirring on a magnetic stirrer PE-6600 (Ecroskhim, Russia). After 1, 3 and 6 h, aliquots of 100 µL were taken from each test tube and added to sterile PBS. 30 µL of the PBS suspension were spread on Mueller–Hinton agar plates. The residual viable bacteria (CFU/mL) were counted after 24 h incubation at 37 °C.

Micro-organisms in PBS only were used as negative controls. Micro-organisms in the presence of CuO and ZnO EEW nanoparticles were used as positive controls. For each sample, two independent experiments with five repetitions for every sample per experiment were performed. Statistical analysis was performed by unpaired Student's *t* test and $p < 0.05$ was considered statistically significant.

3 Results and discussion

Figure 2a shows TEM images of the studied ZnO^{50}–CuO^{50} CNPs. The particles are mostly spherical or close to spherical shape. The distribution of Cu and Zn in particle volume based on the data of elemental analysis is homogenous for some particles, other particles are characterized by the predominance of one of the elements, there are also particles with segregated components with a core–shell or Janus-like structure.

Figure 2b shows TEM images of ZnO^{74}–CuO^{26} CNPs. The particles are mostly spherical. This sample is characterized by the presence of particles mainly enriched with Zn and having a complex shape. The distribution of Cu and Zn in particles is inhomogenous. ZnO^{92}–CuO^{8} CNPs is a set of particles having a spherical, hexagonal and cylindrical shape (Fig. 2c). No copper enriched areas are observed, this can be connected both with homogeneous copper distribution and low copper content which gives response at the background level. ZnO nanoparticles have predominantly faceted shape (Fig. 2d). There are also cubic, hexagonal, oval and less often spherical shaped nanoparticles. CuO nanoparticles are spherical shaped, size ranges from 40 to 120 nm (Fig. 2e).

In the XRD patterns of the CNPs (Fig. 3), the main reflexes correspond to the phases of ZnO (PDF Card No. 01-078-3325), CuO (PDF Card No. 00-002-1040) and, in less extent, Cu_2O (PDF Card No. 01-078-5772). The intensity of the reflexes correlates with Cu–Zn ratio in the samples. The main reflexes observed on the diffractogram ZnO correspond to ZnO phase (PDF Card No. 01-078-3325). The main reflexes observed on the diffractogram CuO correspond to CuO phase (PDF Card No. 00-002-1040) and Cu_2O (PDF Card No. 01-078-5772). Low intensity peaks corresponding to Cu phase are also observed (PDF Card No. 01-071-3671).

The particles being agglomerated, CNPs agglomerates size distributions curves have been obtained. As can be seen, similar distribution curves are characteristic for all samples (Fig. 4). Based on the form of curves the particles slight agglomeration can be assumed. Agglomerates average size is 74 nm for ZnO^{50}–CuO^{50}, 85 nm for ZnO^{74}–CuO^{26}, 102 nm for ZnO^{92}–CuO^{8}. CuO and ZnO nanoparticles agglomerates average size is 50 and 82 nm respectively.

Zeta potential is one of the important characteristics of nanoparticles which inhibit bacteria viability. Positively charged particles are quickly bound to the negatively charged bacterial membrane due to electrostatic interaction resulting in change membrane permeability in virtue of depolarization [22].

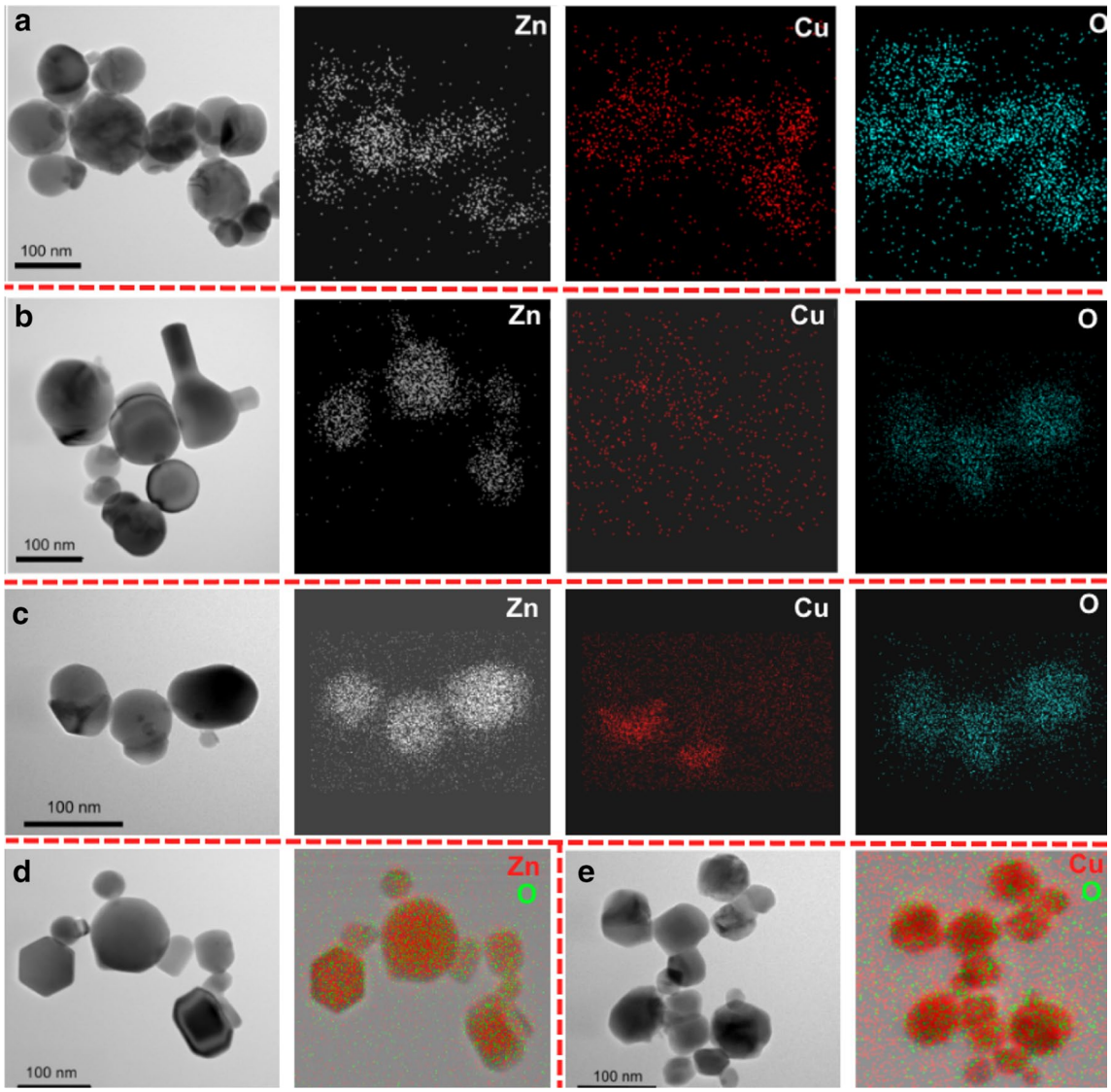

Fig. 2 TEM-image of nanoparticles: **a** ZnO^{50}–CuO^{50}, **b** ZnO^{74}–CuO^{26}, **c** ZnO^{92}–CuO^{8}, **d** ZnO, **e** CuO

Figure 5 shows the curves of changes in zeta potential of the nanoparticles as a function of pH value. As can be seen, zeta potential varies from ~ 40 mV in acidic condition to ~ − 38 mV in basic condition. Isoelectric point (IEP) of ZnO^{50}–CuO^{50} is 9.7; ZnO^{74}–CuO^{26}—9.3; ZnO^{92}–CuO^{8}—9.6. Zeta potential measured at 25 °C and pH 7 has positive values. These values are ~ 41 mV for ZnO^{50}–CuO^{50}, 38 mV for ZnO^{74}–CuO^{26} and 37 mV for ZnO^{92}–CuO^{8}. Thus, CNPs zeta potential remains positive in the entire pH range of bacteria viability. ZnO and CuO nanoparticles prepared in analogous conditions have similar characteristics. Zeta potential of ZnO nanoparticles at 25 °C and pH 7 is ~ 35 mV, IEP being 9.7, zeta potential of CuO nanoparticles at 25 °C and pH 7 is 23 mV, IEP being 9.3.

3.1 Antibacterial activity

Nanoparticles antibacterial activity was studied by agar diffusion test method against Gram-positive bacteria *E. coli* A and Gram- negative bacteria MRSA (Fig. 6). Statistical analysis showed the measured diameters of inhibition growth zones around wells containing CNPs to be larger than those around wells containing ZnO and CuO nanoparticles. As seen in Table 2 bacteria inhibition growth zone diameter for ZnO and CuO nanoparticles does not exceed 12 mm. The maximum bacteria inhibition growth zone diameter was demonstrated in case of ZnO^{5}–CuO^{50} and ZnO^{74}–CuO^{26}—16.4 and 18.3 mm respectively.

Nanopaticles antibacterial activity has been confirmed additionally by micro dilution assay against MRSA. As seen in Fig. 7 all particles tested possess antibacterial

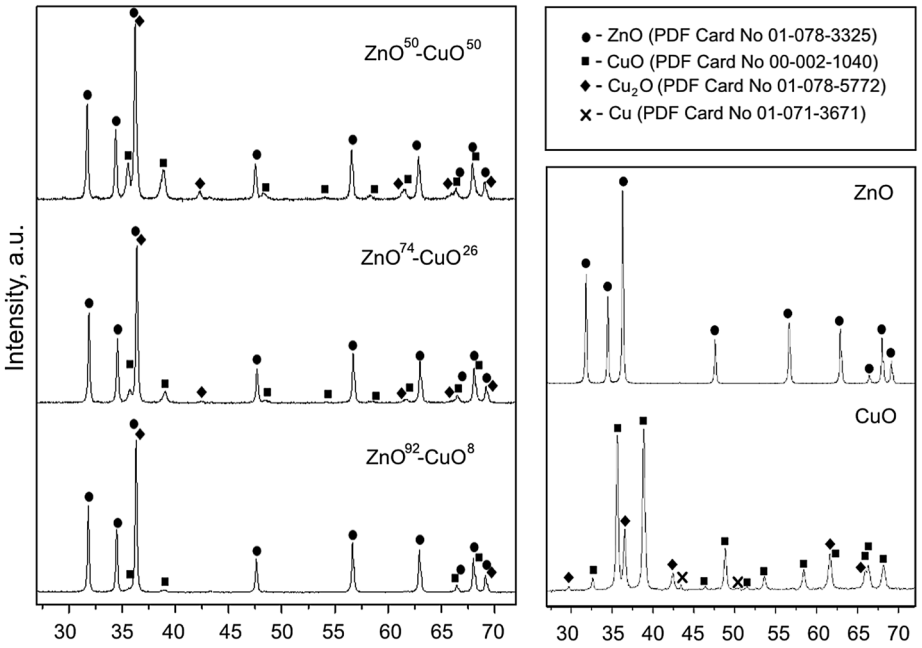

Fig. 3 X-ray diffraction pattern of the nanoparticles

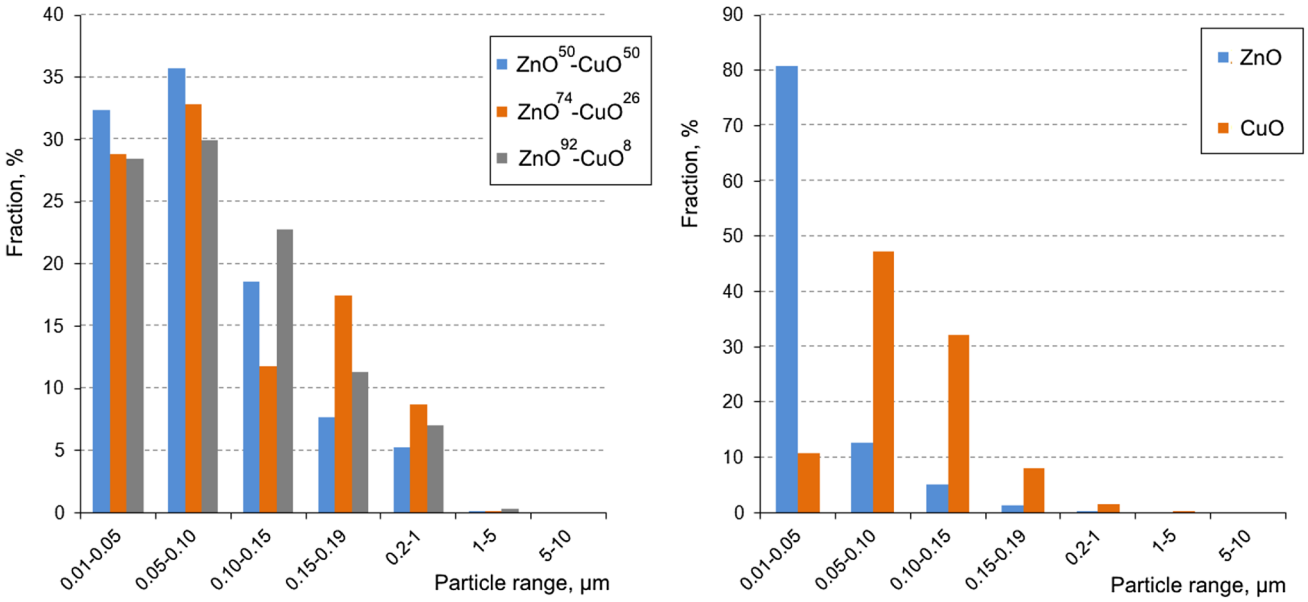

Fig. 4 Agglomerate particle size distribution

activity against MRSA, the bactericidal effect was observed in 6 h exposition. As can be seen from the histogram in Fig. 7a, ZnO^{74}–CuO^{26} considerably reduced the number of bacteria already after 1 h exposure. Similar effect for ZnO^{50}–CuO^{50} was observed only after 3 h exposure. The least antibacterial activity among CNPs was demonstrated by $ZnO^{92}CuO^{8}$, whose activity was comparable with that of ZnO nanoparticles.

Main factor which can be thus associated with CNPs antibacterial activity is copper cation release into surrounding medium. Copper cations demonstrate antibacterial activity against a wide range of bacteria such as *S. aureus, Salmonella enteric, Campylobacter jejuni, E. coli u Listeria monocytogenes* [23]. Currently, copper has been registered by the US Environmental Protection Agency as the first and only metal with antibacterial properties. Raffi et al. [24] explained the antibacterial effect of copper nanoparticles to be due to copper cation release followed by the induction of intracellular reactive oxygen species. Li et al. [25] showed that 10 ppm copper results in decrease growth of *E. coli* by 90

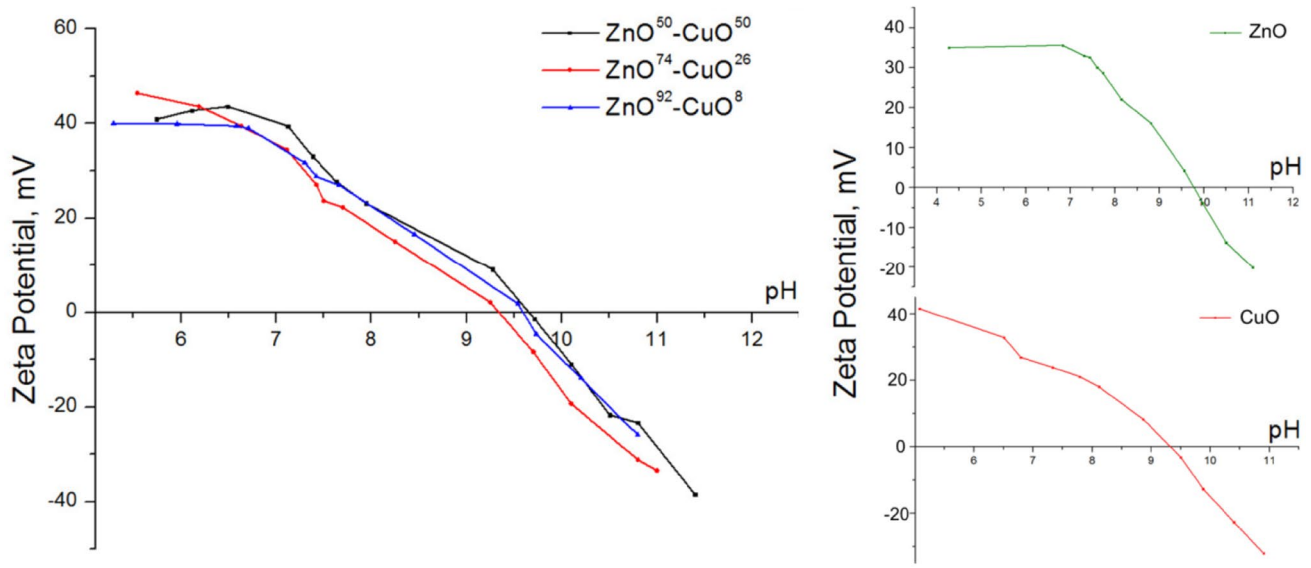

Fig. 5 Zeta potential curves of nanoparticles

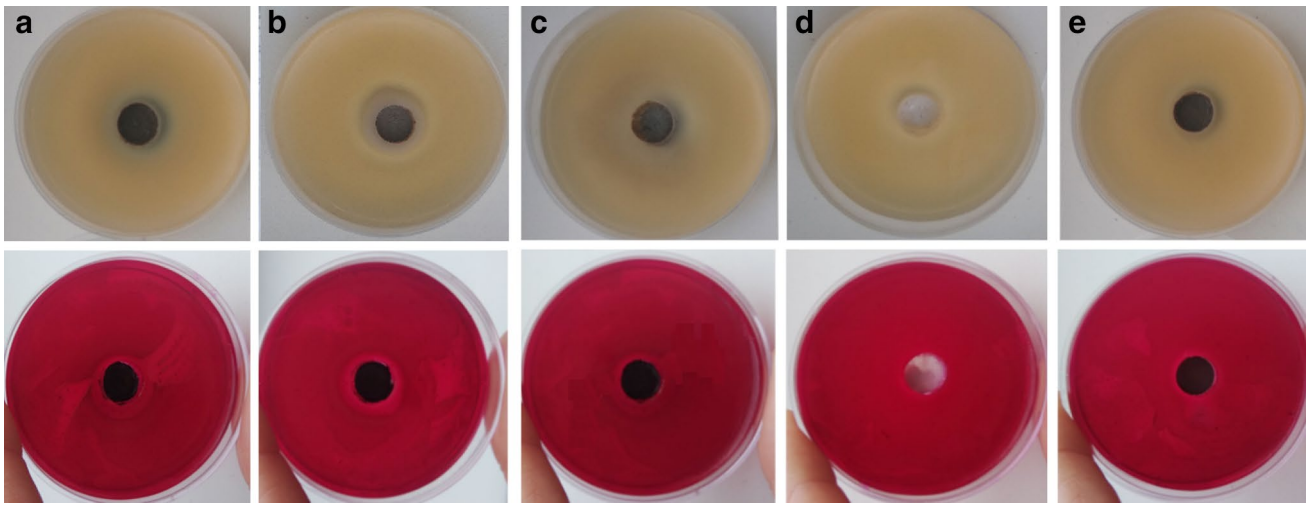

Fig. 6 Photographs of semi-solid agar plates inoculated with *Escherichia coli* (**a**) and MRSA (**b**) showing a clear zone of growth inhibition using nanoparticles by the agar-well diffusion method: **a** ZnO^{50}–CuO^{50}, **b** ZnO^{74}–CuO^{26}, **c** $ZnO^{92}CuO^{8}$, ZnO (**d**) and CuO (**e**) nanoparticles used as a positive control

Table 2 Antibacterial activity of nanoparticles

Nanoparticles	Tested organisms			
	Escherichia coli ATCC 25922		MRSA ATCC 43300	
	IZ	± SD	IZ	± SD
ZnO^{50}–CuO^{50}	16.4	0.1	13.7	0.2
ZnO^{74}–CuO^{26}	15.6	0.3	18.3	0.3
$ZnO^{92}CuO^{8}$	13.7	0.3	11.9	0.3
ZnO	11.9	0.2	11.3	0.1
CuO	10.8	0.2	11.9	0.2

IZ diameter of inhibition zone (mm), *SD* standard deviation

percent after 3 h exposure. Macrocyclic copper complexes inhibited MRSA growth in the concentration of copper cations realased ranged from 6.25 to 12.5 µg/mL.

As illustrated in Fig. 8, the release of the metal cations from metal oxide nanoparticles takes place which can be the key factor of the antibacterial activity. Whilst in case of CNP, the copper cation released concentration during the exposure time from 30 min to 24 h does no exceed 1 µg/mL. It follows that there is not enough copper cation in the medium for rapid bacteria inactivation.

The highest concentration of zinc cations released was observed for ZnO nanoparticles, which did not exhibit high

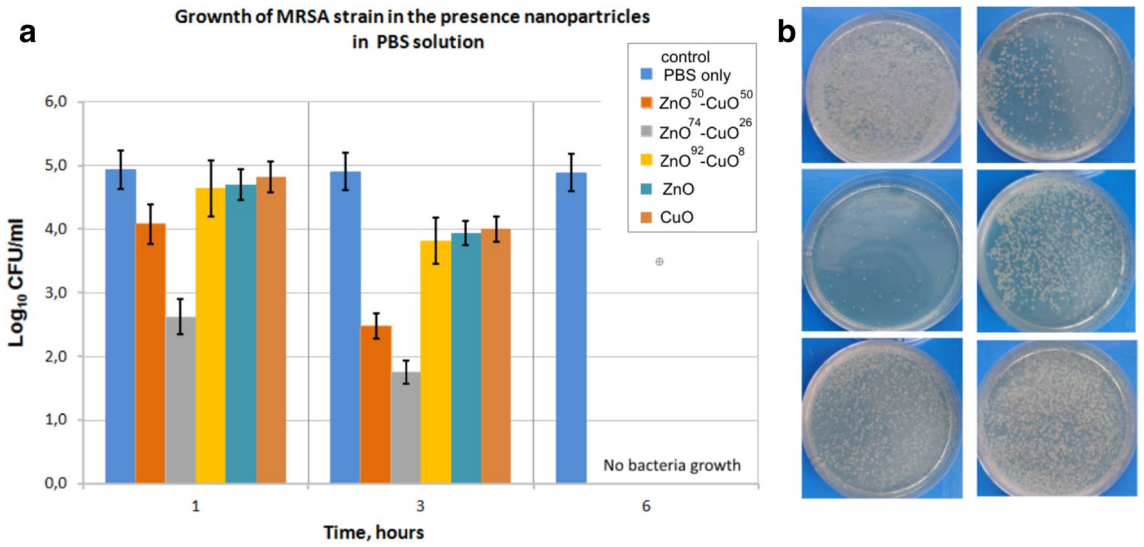

Fig. 7 Results of time-kill assay of nanoparticles against MRSA (**a**) and photographs of agar plates after 1 h exposure nanoparticles with MRSA (**b**)

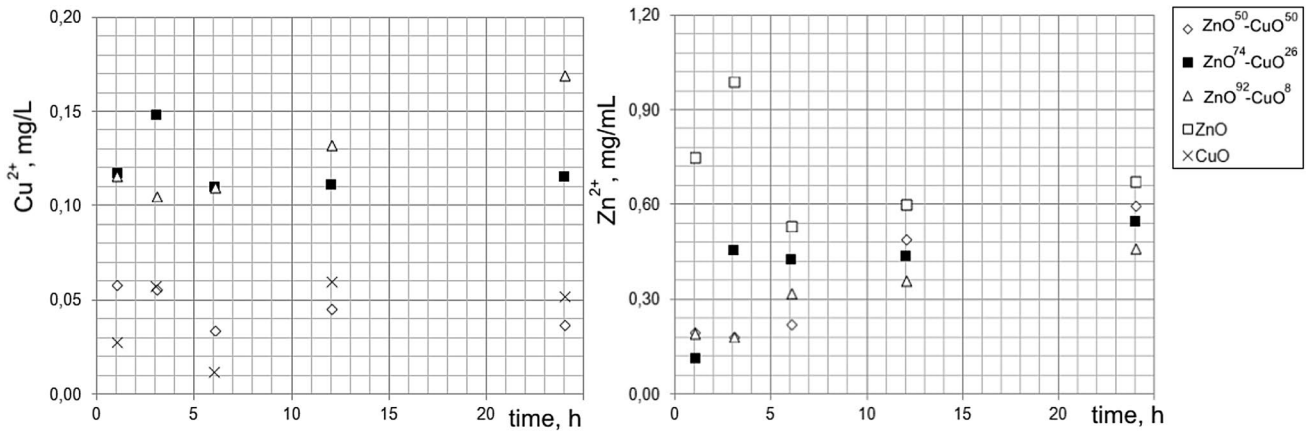

Fig. 8 The release of $Cu^{2+}$and Zn^{2+} ions into the surrounding medium

antibacterial activity. The mechanism of action of ZnO nanoparticles and zinc cations is complex and includes multiple metabolic pathways [26].

On the contrary, CNPs are more active than monometal oxide nanoparticles. Two possible mechanisms of the antibacterial activity thus can be suggested. CNPs with the higher zeta potential interact electrostatically with bacterial cell wall resulting in membrane disruption followed by bacterial cell death. Another possible mechanism may include release of metal cations from nanoparticles, action of the cation on bacterial cell followed by the cell membrane depolarization [27]. The results of the study point to the importance of deeper experimental investigation to interpretate antibacterial activity mechanisms including at molecular level.

4 Conclusion

The results obtained in this study demonstrate that it is possible by electrical explosion of copper and zinc wires in argon atmosphere, to obtained CuO–ZnO nanopartilces with different components ratios and positive surface charge. We've also demonstrated that the synthesized nanoparticles possess high antibacterial activity against both gram-negative (*E. coli*) and high resistant gram-positive (MRSA) bacterial strains and can completely inhibit the growth of these microorganisms without substantial release of copper and zinc ions. The bacterial killing capability of the nanoparticles is believed to be due electrostatic interaction resulting in change membrane

permeability in virtue of depolarization. These results suggest that CuO–ZnO nanopartilces are a promising antibacterial agent for biomedical applications.

Acknowledgements The synthesis and characterization of flower-shaped micro/nanostructures were produced under the financial support of the Russian Science Foundation (Project No. 17-19-01319).

References

1. J.S. Chapman, Characterizing bacterial resistance to preservatives and disinfectants. Int. Biodeteriorat. Biodegradat. (1998). https://doi.org/10.1016/S0964-8305(98)00025-0
2. F. Baquero, J.L. Martínez, R. Cantón, Antibiotics and antibiotic resistance in water environments. Curr. Opin. Microbiol. (2008). https://doi.org/10.1016/j.copbio.2008.05.006
3. J.L. Martínez, Antibiotics and antibiotic resistance genes in natural environments. Science (2008). https://doi.org/10.1126/science.1159483
4. R. Nordmann, T. Naas, N. Fortineau, L. Poirel, Superbugs in the coming new decade; multidrug resistance and prospects for treatment of *Staphylococcus aureus*, *Enterococcus* spp. and *Pseudomonas aeruginosa* in 2010. Curr. Opin. Microbiol. (2007). https://doi.org/10.1016/j.mib.2007.07.004
5. K. Gold, B. Slay, M. Knackstedt, A.K. Gaharwa, Antimicrobial activity of metal and metal-oxide based nanoparticles. Adv. Ther. (2018). https://doi.org/10.1002/adtp.201700033
6. S.P. Murzin, A.B. Prokofiev, A.I. Safin, E.E. Kostriukov, Creation of ZnO-based nanomaterials with use synergies of the thermal action and laser-induced vibrations. (2018). doi.org/10.1088/1742-6596/1096/1/012150
7. H.D.M. Follmann, A.F. Naves, R.A. Araujo, V. Dubovoy, X. Huang, T. Asefa, N.O. Oliveira, Hybrid materials and nanocomposites as multifunctional biomaterials. Curr. Pharm. Des. (2017). https://doi.org/10.2174/1381612823666170710160615
8. A. Bumajdad, M. Madkour, Y.K. Abdel-Moneam, M. El-Kemary, Nanostructured mesoporous Au/TiO_2 for photocatalytic degradation of a textile dye: the effect of size similarity of the deposited Au with that of TiO_2 pores. J. Mater. Sci. (2014). https://doi.org/10.1007/s10853-013-7861-0
9. S. Stankic, S. Suman, F. Haque, J. Vidic, Pure and multi metal oxide nanoparticles: synthesis, antibacterial and cytotoxic properties. J. Nanobiotechnol. (2016). https://doi.org/10.1186/s12951-016-0225-6
10. W.M. Obina, A. Supriyanto, S. Sumardiasih, T.Y. Septiawan, Fabrication and variation layers of Cu/TiO2 nanocomposite and its applications in dye-sensitized solar cell (DSSC). (2017). doi.org/10.1088/1742-6596/795/1/012029
11. A.S. Lozhkomoev, A.V. Pervikov, O.V. Bakina, S.O. Kazantsev, I. Gotman, Synthesis of antimicrobial AlOOH–Ag composite nanostructures by water oxidation of bimetallic Al–Ag nanoparticles. RSC Adv. (2018). https://doi.org/10.1039/C8RA04173C
12. H. Liu, J. Feng, W. Jie, A review of noble metal (Pd, Ag, Pt, Au)–zinc oxide nanocomposites: synthesis, structures and applications. J. Mater. Sci. (2017). https://doi.org/10.1007/s10854-017-7612-0
13. D. Das, B.C. Nath, P. Phukon, S.K. Dolui, Synthesis and evaluation of antioxidant and antibacterial behavior of CuO nanoparticles. Colloids Surf. B (2013). https://doi.org/10.1016/j.colsurfb.2012.07.002
14. N. Jones, B. Ray, K.T. Ranjit, A.C. Manna, Antibacterial activity of ZnO nanoparticle suspensions on a broad spectrum of microorganisms. FEMS Microbiol. Lett. (2008). https://doi.org/10.1111/j.1574-6968.2007.01012.x
15. M. Carbone, R. Briancesco, L. Bonadonna, Antimicrobial power of Cu/Zn mixed oxide nanoparticles to *Escherichia coli*. Environ. Nanotechnol. Monit. Manag. (2017). https://doi.org/10.1016/j.enmm.2017.01.005
16. D.M. Fernandes, R. Silva, A.W. Hechenleitner, E. Radovanovic, M.C. Melo, E.G. Pineda, Synthesis and characterization of ZnO, CuO and a mixed Zn and Cu oxide. Mater. Chem. Phys. (2009). https://doi.org/10.1063/1.4821253
17. K. Varaprasad, Co-assembled ZnO (shell)–CuO (core) nanooxide materials for microbial protection. Phosphorus Sulfur Silicon Relat. Elem. (2018). https://doi.org/10.1080/10426507.2017.1417301
18. N. Widiarti, J.K. Sae, S. Wahyuni, Synthesis CuO–ZnO nanocomposite and its application as an antibacterial agent. (2017). doi.org/10.1088/1757-899X/172/1/011002
19. D. Malwal, P. Gopinath, Efficient adsorption and antibacterial properties of electrospun CuO–ZnO composite nanofibers for water remediation. J. Hazard. Mater. (2017). https://doi.org/10.1016/j.jhazmat.2016.09.050
20. C. Wang, L. Yue, S. Wang, Y. Pu, X. Zhang, X. Hao, S. Chen, Role of electric field and reactive oxygen species in enhancing antibacterial activity: a case study of 3D Cu foam electrode with branched CuO–ZnO NWs. J. Phys. Chem. C (2018). https://doi.org/10.1021/acs.jpcc.8b08232
21. R. Mohammadi-Aloucheh et al., Green synthesis of ZnO and ZnO/CuO nanocomposites in *Mentha longifolia* leaf extract: characterization and their application as anti-bacterial agents. J. Mater. Sci. (2018). https://doi.org/10.1007/s10854-018-9487-0
22. D. Paul, S. Neogi, Synthesis, characterization and a comparative antibacterial study of CuO, NiO and CuO–NiO mixed metal oxide. Mater. Res. Express (2019). https://doi.org/10.1088/2053-1591/ab003c
23. C.E. Santo, N. Taudte, D.H. Nies, G. Grass, Contribution of copper ion resistance to survival of *Escherichia coli* on metallic copper surfaces. Appl. Environ. Microbiol. (2007). https://doi.org/10.1128/AEM.01938-07
24. M.M. Raffi, S. Mehrwan, T.M. Bhatti, J.I. Akhter, A. Hameed, W. Yawar, Investigations into the antibacterial behavior of copper nanoparticles against *Escherichia coli*. Ann. Microbiol. (2010). https://doi.org/10.1007/s13213-010-0015-6
25. H.H. Li, Q.S. Chen, J.W. Zhao, K. Urmila, Enhancing the antibacterial activity of natural extraction using the synthetic ultrasmall metal nanoparticles. Sci. Rep. **5**, 11033 (2015). https://doi.org/10.1038/srep11033
26. U. Kadiyala, E.S. Turali-Emre, J.H. Bang, N.A. Kotov, J.S. VanEpps, Unexpected insights into antibacterial activity of zinc oxide nanoparticles against methicillin resistant *Staphylococcus aureus* (MRSA). Nanoscale (2018). https://doi.org/10.1039/C7NR08499D
27. A.K. Chatterjee, R. Chakraborty, T. Basu, Mechanism of antibacterial activity of copper nanoparticles. Nanotechnology **25**, 135101 (2014). https://doi.org/10.1088/0957-4484/25/13/135101